

Shape changes in ^{79}Kr G.D. Johns, J. Döring, J.W. Holcomb,* T.D. Johnson,† M.A. Riley, G.N. Sylvan, P.C. Womble,‡
V.A. Wood, and S.L. Tabor*Department of Physics, Florida State University, Tallahassee, Florida 32306*

(Received 22 June 1994)

High-spin states in ^{79}Kr were studied using the $^{65}\text{Cu}(^{18}\text{O},p3n)$ reaction at 65 MeV at the Florida State University Tandem-LINAC facility. Prompt γ - γ coincidences were observed using the Pitt-FSU detector array. Twelve new states were found, along with 19 new transitions. The yrast positive- and negative-parity bands were extended up to spins of $(45/2^+)$ and $(31/2^-)$, respectively. Spin assignments were made based on directional correlation of oriented nuclei ratios whenever possible. A cranked-shell-model analysis shows some indication for a second band crossing in the positive-parity band at $\hbar\omega \approx 0.75$ MeV. This crossing, probably due to an aligned $g_{9/2}$ neutron pair, occurs with a much larger band interaction than the first $g_{9/2}$ proton crossing. An increase in signature splitting above $\hbar\omega \approx 0.75$ MeV and a return of large alternations in the $B(M1)/B(E2)$ ratio is consistent with the theoretically predicted return to a nearly oblate shape.

PACS number(s): 23.20.Lv, 27.50.+e, 29.30.Kv

I. INTRODUCTION

Nuclei in the f - p - g shell exhibit a wide range of shapes and are particularly sensitive to the polarizing influences of unpaired nucleons. A very dramatic change has been observed, e.g., in the positive-parity yrast bands of the $N = 43$ isotones ^{79}Kr [1,2], ^{81}Sr [3], and in the $N = 45$ nuclei ^{81}Kr [4] and ^{83}Sr [5]. Above a spin of about $\frac{21}{2}\hbar$ the large signature splitting vanishes and $M1$ transitions become very strong. This has been interpreted as a shape transformation from a near-oblate to a near-prolate shape caused by the alignment of a pair of $g_{9/2}$ protons. The same calculations [2] predict another equally dramatic shape change, a return to a near-oblate shape in ^{79}Kr at even higher spins. However, no experimental information was available on the behavior of the band at spins above $\frac{29}{2}\hbar$.

Most of the present understanding of the structure of ^{79}Kr has been accumulated since the early 1980s. The first evidence for a decoupled rotational band in ^{79}Kr came from a ^{10}B induced fusion-evaporation reaction [6]. The band was placed atop a $\frac{9}{2}^+$ level established earlier from a β^+ decay study [7]. Several investigations [1,2,8,9] were subsequently made using α -induced reactions. These studies extended the level scheme up to levels with spins and parities of $\frac{23}{2}^-$ and $\frac{27}{2}^+$ with additional tentative levels at 4708 and 5523 keV, respectively. The later work [1,2] revealed the rather unusual band cross-

ing in the positive-parity band discussed above and also a high-lying high- K band built on a $(\frac{17}{2}^-)$ state at 2857 keV. The lifetimes of many of the states in the known level scheme were measured using both α -induced [1,2] and heavy-ion [10] reactions.

The present work was undertaken primarily to look for evidence of a second possible band crossing and shape change in the yrast band of ^{79}Kr . Increased sensitivity to explore higher in the level scheme was provided by a modern Compton-suppressed Ge-detector array and by the greater angular momentum available from a heavy-ion induced reaction. Evidence for a second band crossing in the nearby nucleus ^{83}Sr has been presented in Ref. [5], and during the course of this investigation, a preliminary report [11] on a similar structure in the nucleus ^{81}Sr became available. These studies have provided insights into the shape changes driven by increasing numbers of unpaired nucleons.

II. EXPERIMENTAL TECHNIQUES

High-spin states in ^{79}Kr were studied via the fusion evaporation reaction $^{65}\text{Cu}(^{18}\text{O},p3n)$. The Florida State University Tandem-LINAC facility was used to provide the 65 MeV ^{18}O beam which was produced from H_2^{18}O in the sputter ion source. The 0.6 mg/cm² thick self-supporting copper target was enriched to 99% in ^{65}Cu .

The joint Pitt-FSU detector array [12] used in this experiment consisted of nine Compton-suppressed high-purity Ge detectors and a 28-element Bismuth-Germanate (BGO) sum energy and multiplicity filter. Three of the Ge detectors were located 90° relative to the beam axis, two were positioned at 35°, and the remaining four detectors were placed at 145°. Internal energy calibrations, which take into account Doppler shifting, were made using strong γ rays from ^{76}Br , ^{78}Kr , ^{79}Rb , ^{80}Kr , and ^{79}Kr . All of these nuclei were produced during the

*Present address: Martin Marietta Information Systems, Mail Point 800, Orlando, FL 32825.

†Present address: Department of Physics, University of Notre Dame, Notre Dame, IN 46556.

‡Present address: Oak Ridge National Laboratory, Mail Stop 6388, Oak Ridge, TN 37830.

irradiation of ^{65}Cu with ^{18}O at 65 MeV. The calibration was performed by making a linear least-squares fit of the energies to the channel numbers.

Approximately 1.8×10^8 γ - γ coincidences were collected on magnetic tape and then sorted [13] into a 2500 channel triangular array with a dispersion of 0.8 keV per channel. Coincidence spectra were obtained by gating on the triangular array and subtracting a fraction of the total projection as background. From these gates, the γ -ray intensities and energies were obtained and were used to deduce the level scheme.

The coincidence data were also sorted into a two-dimensional square array. This array was constructed by sorting the 90° detector information onto one axis and either the 35° or the 145° detector information onto the other axis. Gates from this array on known $\Delta I=2$ transitions were used to determine multipolarities of the γ -ray transitions to assist in assigning spins by calculating directional correlation of oriented nuclei (DCO) ratios whenever possible according to

$$R_{\text{DCO}} = \frac{I_\gamma(\text{ at } 35^\circ, 145^\circ \text{ gated by } \gamma_G \text{ at } 90^\circ)}{I_\gamma(\text{ at } 90^\circ \text{ gated by } \gamma_G \text{ at } 35^\circ, 145^\circ)} \quad (1)$$

The DCO ratios for stretched electric quadrupole ($E2$) transitions are expected to have values close to 1, while $\Delta I = 1$ transitions can have values ranging from 0 to 2 depending on the multipole mixing ratio δ . If the $E2/M1$ mixing ratio is small, then the DCO ratio is expected [3] to be near 0.5. Similarly, for stretched $E1$ transitions a DCO ratio of 0.5 is expected. As in all fusion-evaporation experiments, the spin assignments are based on the DCO ratios, the expectation that primarily yrast and near-yrast states are populated, and the systematics of rotational bands.

III. THE LEVEL SCHEME

The level scheme shown in Fig. 1 was deduced from coincidence spectra generated by gating on the square and triangular arrays. Level energies, relative intensities, branching ratios, spins, and DCO ratios are given in Table I. In the present work, 19 new transitions were identified which lead to 12 new excited states.

A. The positive-parity band

The favored signature ($\alpha = +\frac{1}{2}$) positive-parity yrast band was previously known up to the $\frac{21}{2}^+$ level at 3146 keV [8,9] and has since been extended [2] up to the tentative 5523 keV level. The present work has confirmed this result and has extended the band up to the $(\frac{45}{2}^+)$ 11 822 keV level. Figure 2 shows the sum of background-corrected coincidence spectra gated on the 827, 1026, and 1144 keV transitions. The 1367, 1510, 1639, and 1782 keV transitions have been added to the yrast sequence. The first three transitions are $E2$ in character based on DCO ratios close to unity. Since no DCO ratio could

be measured for the 1782 keV transition, the spin of the 11 822 keV level is tentatively assigned $(\frac{45}{2}^+)$ based on systematics.

The $\alpha = -\frac{1}{2}$ signature-partner band was previously known [2] up to the $\frac{27}{2}^+$ 4900 keV level. This band has been confirmed in the present work and extended to the 9704 keV $(\frac{39}{2}^+)$ state. Spin and parity assignments were made for the states up to the $\frac{35}{2}^+$ state based on the DCO ratios for the deexciting γ rays. The highest state has been shown with a dashed line in the level scheme because the weakness of the 1800 keV line makes exact determination of its coincidence relations difficult.

The $\Delta I = 1$ transition sequence was extended from the 5524 keV level to the $\frac{37}{2}^+$ 8401 keV level with the exception of the decay from the $\frac{35}{2}^+$ 7904 keV level. The DCO ratios of the 624 and 641 keV transitions imply $\Delta I = 1$ decays and support our spin assignments. The large DCO ratio of the 497 keV transition would imply a large $M1/E2$ mixing ratio unlike those of the other $\Delta I = 1$ decays in the band. In addition, a new $\Delta I = 1$ transition was observed between the 3146 and 2980 keV levels.

B. The yrast negative-parity band

The lowest $\alpha = -\frac{1}{2}$ signature sequence was previously known [2] up to the $(\frac{23}{2}^-)$ 4087 keV level. The present work confirms and extends this band up to the $(\frac{31}{2}^-)$ 6446 keV level. Part of a relevant background-corrected coincidence spectrum is shown in Fig. 3. DCO ratios for the two new transitions can be found in Table I. Spin assignments for the $\frac{23}{2}^-$ and $\frac{27}{2}^-$ levels were provided by DCO ratios close to unity, consistent with stretched electric quadrupole transitions. The DCO ratio for the 1281 keV decay from the 6446 keV level was measured to be somewhat larger than one, so a tentative value of $(\frac{31}{2}^-)$ was assigned to that level.

The signature-partner band ($\alpha = +\frac{1}{2}$) was confirmed up to the 4709 keV level, and the spin of the 4709 level has been determined to be $\frac{25}{2}^-$ from the DCO ratio of the 1053 keV transition. An additional 5994 keV level has been found from our coincidences with a tentative $\frac{29}{2}^-$ assignment. Moreover, the previous tentatively assigned [2] 587 keV $\Delta I = 1$ transition was confirmed, and a new 394 keV $\Delta I = 1$ decay was added.

C. Other negative-parity bands

The ground-state band was previously known [2] up to the 3383 keV $(\frac{19}{2}^-)$ level. All of these levels have been observed in the present work including the weak 965 – 967 keV coincidence pair. The previous tentatively assigned spin of $\frac{17}{2}^-$ to the 2930 keV level has been confirmed based on a DCO ratio of 0.99 for the 1014 keV γ ray. A new tentative 4063 keV level has been added to the $\alpha = +\frac{1}{2}$ sequence with an assignment of $(\frac{21}{2}^-)$.

Furthermore, weak coincidences of the 201 and 476 keV γ rays with the 183 keV line have been observed confirming the lowest members of a known [2] negative-parity band, but no new information could be added. There-

fore, this band has been omitted from the level scheme given in Fig. 1.

A high-lying decay sequence based on a ($\frac{17}{2}^-$) 2857 keV level was reported in Ref. [2]. The sequence consists of

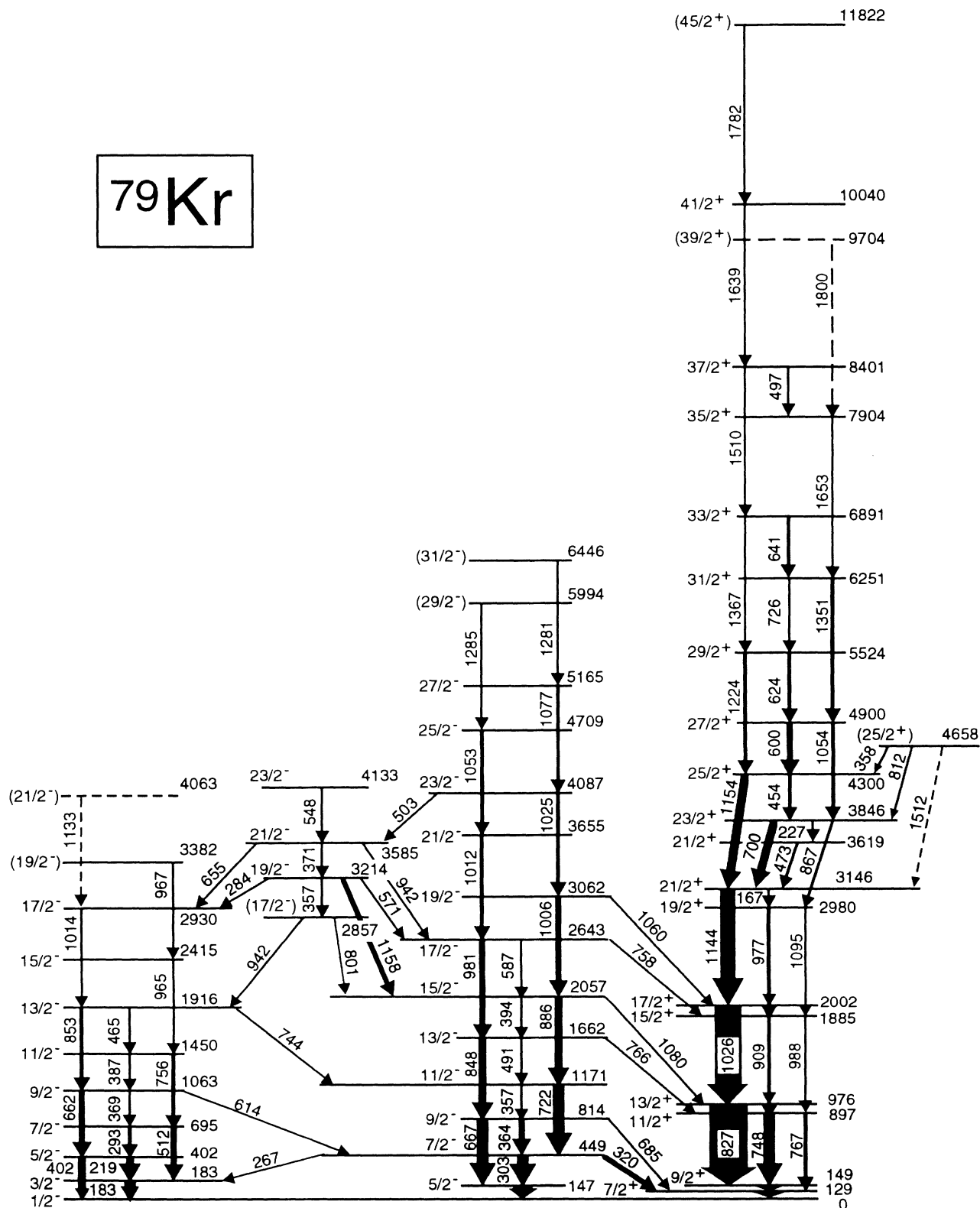


FIG. 1. The level scheme for ^{79}Kr as deduced from the present work.

$\Delta I = 1$ transitions with no $\Delta I = 2$ crossover transitions and was confirmed in the present work. In addition to the known transitions, weak γ rays at 1081, 1230, and 1273 keV have been seen in various coincidence gates; however, they could not be placed unambiguously in this part of the level scheme.

IV. DISCUSSION

The behavior of the yrast positive-parity band is rather regular at high spins, showing a more gradual change than that seen around the $\frac{21}{2}^+$ states. As can be seen in Fig. 1, there is a gradual increase in the signature

TABLE I. Energies, relative intensities, branching ratios, and DCO ratios for transitions in ^{79}Kr .

E_{lev} (keV)	E_{γ} (keV)	I_i^{π}	I_f^{π}	I_{γ}^a	B.R.(%)	R_{DCO}	E_{lev} (keV)	E_{γ} (keV)	I_i^{π}	I_f^{π}	I_{γ}^a	B.R.(%)	R_{DCO}
129.4	129.4(4)	$7/2^+$	$1/2^-$		100			1094.6(2)	$19/2^+$	$15/2^+$	6(2)	38(9)	
146.7	146.7(3)	$5/2^-$	$1/2^-$		100		3062.0	1005.5(2)	$19/2^-$	$15/2^-$	29(2)	97(3)	1.07(7)
148.6	19.2 ^b	$9/2^+$	$7/2^+$		100			1060.1(8)	$19/2^-$	$17/2^+$	1	3(2)	
182.7	182.7(2)	$3/2^-$	$1/2^-$	47(4)	100		3146.4	166.6(3)	$21/2^+$	$19/2^+$	2(1)	3(1)	
401.7	219.0(2)	$5/2^-$	$3/2^-$	23(2)	49(5)	0.86(13)		1144.2(2)	$21/2^+$	$17/2^+$	68(1)	97(1)	1.02(7)
	401.8(2)	$5/2^-$	$1/2^-$	24(4)	51(5)	0.82(8)	3214.2	283.9(3)	$19/2^-$	$17/2^-$	2(1)	11(4)	
449.4	267.0(3)	$7/2^-$	$3/2^-$	3(1)	4(1)			356.5(3)	$19/2^-$	$(17/2^-)$	2(1)	8(4)	
	302.6(2)	$7/2^-$	$5/2^-$	52(4)	69(3)	0.98(4)		570.9(4)	$19/2^-$	$17/2^-$	2(1)	9(4)	
	320.0(2)	$7/2^-$	$7/2^+$	20(2)	27(2)	1.13(4)		1157.7(3)	$19/2^-$	$15/2^-$	15(2)	72(6)	1.07(5)
694.5	292.7(2)	$7/2^-$	$5/2^-$	12(2)	44(5)	0.86(9)	3382	967(1)	$(19/2^-)$	$15/2^-$	2(1)	100	
	512.0(3)	$7/2^-$	$3/2^-$	15(2)	56(5)	0.61(12)	3585.0	371.0(2)	$21/2^-$	$19/2^-$	8(2)	47(7)	0.52(2)
813.9	364.1(3)	$9/2^-$	$7/2^-$	4(1)	7(2)			654.9(4)	$21/2^-$	$17/2^-$	4(1)	24(5)	
	667.2(2)	$9/2^-$	$5/2^-$	46(3)	82(2)	0.99(6)		941.8(5)	$21/2^-$	$17/2^-$	5(1)	29(6)	
	684.5(2)	$9/2^-$	$7/2^+$	6(1)	11(2)		3619.4	473.0(2)	$21/2^+$	$21/2^+$	5(1)	100	
896.6	748.0(2)	$11/2^+$	$9/2^+$	25(5)	83(9)		3655.3	1012.2(3)	$21/2^-$	$17/2^-$	26(4)	100	
	767.2(2)	$11/2^+$	$7/2^+$	5(3)	17(9)		3846.4	227.1(3)	$23/2^+$	$21/2^+$	2(1)	6(3)	
975.9	79.3(8)	$13/2^+$	$11/2^+$	1	1(0.5)			700.0(2)	$23/2^+$	$21/2^+$	28(1)	80(3)	0.50(7)
	827.3(2)	$13/2^+$	$9/2^+$	100 ^c	99(0.5)	1.05(5)		867.1(4)	$23/2^+$	$19/2^+$	5(1)	14(3)	1.01(16)
1063.2	368.6(4)	$9/2^-$	$7/2^-$	3(1)	14(4)		4063	1133(1)	$(21/2^-)$	$17/2^-$	2(1)	100	
	613.5(7)	$9/2^-$	$7/2^-$	1	5(2)		4087.4	502.5(4)	$23/2^-$	$21/2^-$	2(1)	13(6)	
	661.5(2)	$9/2^-$	$5/2^-$	17(1)	81(4)	1.28(9)		1025.4(6)	$23/2^-$	$19/2^-$	13(3)	87(6)	1.06(11)
1171.0	356.8(3)	$11/2^-$	$9/2^-$	2(1)	4(2)		4132.7	547.7(4)	$23/2^-$	$21/2^-$	3(1)	100	
	721.6(2)	$11/2^-$	$7/2^-$	45(2)	96(2)	0.99(4)	4299.9	453.8(3)	$25/2^+$	$23/2^+$	13(2)	30(4)	0.55(9)
1450.2	386.9(4)	$11/2^-$	$9/2^-$	1	9(4)			1153.5(2)	$25/2^+$	$21/2^+$	30(2)	70(4)	1.05(8)
	755.9(2)	$11/2^-$	$7/2^-$	10(1)	91(4)	0.97(4)	4658.1	357.7(4)	$(25/2^+)$	$25/2^+$	7(3)	64(13)	0.76(10)
1662.0	490.5(3)	$13/2^-$	$11/2^-$	1	2(1)			811.9(5)	$(25/2^+)$	$23/2^+$	2(1)	18(9)	0.67(26)
	765.7(3)	$13/2^-$	$11/2^+$	3(1)	7(2)			1512(1)	$(25/2^+)$	$21/2^+$	2(1)	18(9)	
	848.1(2)	$13/2^-$	$9/2^-$	40(4)	91(2)	1.02(5)	4708.7	1053.4(3)	$25/2^-$	$21/2^-$	12(1)	100	1.02(13)
1885.1	909.2(2)	$15/2^+$	$13/2^+$	8(3)	53(14)	0.30(12)	4900.1	600.0(2)	$27/2^+$	$25/2^+$	17(2)	63(5)	0.51(4)
	988.3(2)	$15/2^+$	$11/2^+$	7(3)	47(14)			1053.9(3)	$27/2^+$	$23/2^+$	10(2)	37(5)	0.98(6)
1915.6	464.9(6)	$13/2^-$	$11/2^-$	1	7(3)		5164.7	1077.3(5)	$27/2^-$	$23/2^-$	9(1)	100	1.06(4)
	744.2(6)	$13/2^-$	$11/2^-$	1	7(3)		5524.2	624.3(2)	$29/2^+$	$27/2^+$	15(2)	58(6)	0.52(9)
	852.6(2)	$13/2^-$	$9/2^-$	13(2)	87(4)	1.16(10)		1224.0(3)	$29/2^+$	$25/2^+$	11(2)	42(6)	1.00(5)
2002.2	117.1(4)	$17/2^+$	$15/2^+$	1	1(0.5)		5994	1285(2)	$(29/2^-)$	$25/2^-$	5(2)	100	
	1026.3(2)	$17/2^+$	$13/2^+$	95(1)	99(0.5)	0.98(8)	6250.5	726.0(4)	$31/2^+$	$29/2^+$	6(1)	30(5)	
2056.5	394.4(3)	$15/2^-$	$13/2^-$	1	2(1)			1350.7(5)	$31/2^+$	$27/2^+$	14(2)	70(5)	0.99(5)
	885.5(2)	$15/2^-$	$11/2^-$	41(4)	84(4)	0.96(6)	6446.1	1281.4(8)	$(31/2^-)$	$27/2^-$	6(1)	100	1.25(14)
	1079.7(6)	$15/2^-$	$13/2^+$	7(2)	14(4)		6891.1	640.6(2)	$33/2^+$	$31/2^+$	9(2)	53(8)	0.47(8)
2415	965(1)	$15/2^-$	$11/2^-$	5(2)	100			1366.6(5)	$33/2^+$	$29/2^+$	8(2)	47(8)	1.01(5)
2643.1	587.1(6)	$17/2^-$	$15/2^-$	2(1)	5(3)		7904	1013 ^d	$35/2^+$	$33/2^+$	< 1	< 20	
	758.3(3)	$17/2^-$	$15/2^+$	2(1)	5(3)			1653(2)	$35/2^+$	$31/2^+$	4(1)	> 80	0.97(10)
	981.1(2)	$17/2^-$	$13/2^-$	35(3)	90(3)	1.05(6)	8401.1	497.1(4)	$37/2^+$	$35/2^+$	2(1)	22(10)	1.51(42)
2857.4	800.7(6)	$(17/2^-)$	$15/2^-$	2(1)	25(10)			1510.0(8)	$37/2^+$	$33/2^+$	7(2)	78(10)	0.97(6)
	941.8(4)	$(17/2^-)$	$13/2^-$	6(1)	75(10)		9704	1800(4)	$(39/2^+)$	$35/2^+$	2(1)	100	
2929.8	1014.2(4)	$17/2^-$	$13/2^-$	7(3)	100		10 040	1639(2)	$41/2^+$	$37/2^+$	4(1)	100	1.06(8)
2979.5	977.3(2)	$19/2^+$	$17/2^+$	10(2)	62(9)		11 822	1782(3)	$(45/2^+)$	$41/2^+$	3(1)	100	

^aIntensities determined from triangular array. Weak lines with one intensity unit only have an uncertainty of about 60%.

^bTaken from Ref. [7].

^cNormalization.

^dNot observed.

$\hbar\omega \approx 0.5$ MeV. A similar behavior may be anticipated for ^{81}Sr , but the missing $\frac{19}{2}^+$ state prevents a detailed comparison. There is a slight upturn in $J^{(1)}$ for the $\alpha = -\frac{1}{2}$ curve in ^{79}Kr at $\hbar\omega \approx 0.8$ MeV, but the last point is tentative and the corresponding unfavored sequence is not known so high in frequency in the other isotones. Although the $J^{(1)}$ curve for the $\alpha = +\frac{1}{2}$ signature in ^{79}Kr is fairly smooth at high spins, the dynamic moment of inertia $J^{(2)}$ (shown at bottom of Fig. 4) reveals a weak peak at $\hbar\omega \approx 0.75$ MeV. A small rise begins at a similar frequency in the corresponding $J^{(1)}$ curve for ^{83}Zr and perhaps a rise is beginning at the last point known for ^{81}Sr . These features may indicate the population of the predicted [2] 5qp near-oblate $\nu g_{9/2}^3 \pi g_{9/2}^2$ configuration, where a $g_{9/2}$ neutron pair is aligned in addition to the 3qp configuration. If so, the 3qp-5qp band interaction strength is much larger than at the lower 1qp-3qp crossing.

A band crossing at $\hbar\omega \approx 0.75$ MeV with large interaction strength could account for the rising alignment curve for the $\alpha = +\frac{1}{2}$ band in ^{79}Kr shown in Fig. 5. Both this and the previously established alignment at $\hbar\omega \approx 0.55$

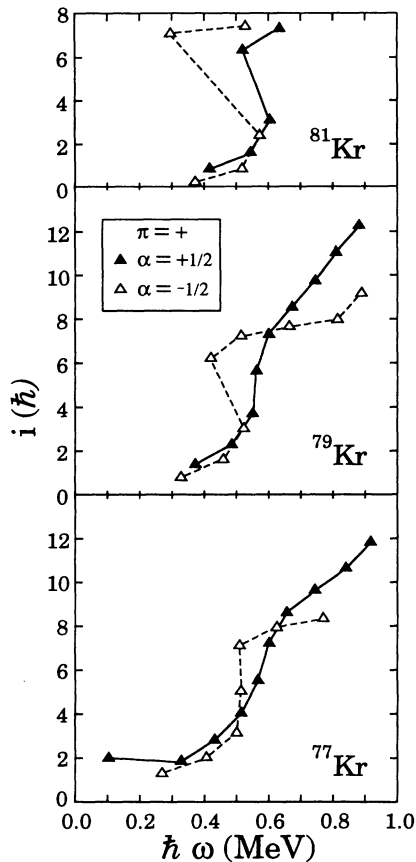


FIG. 5. Aligned angular momentum i versus rotational frequency $\hbar\omega$ for the yrast positive-parity bands in ^{81}Kr [4], ^{79}Kr , and ^{77}Kr [19,21,22]. Harris parameters $J_0 = 11 \hbar^2/\text{MeV}$ and $J_1 = 0 \hbar^3/\text{MeV}^4$ were used for the reference rotor. The positive-parity band of ^{81}Kr has been included even though the $E2$ transitions in the region above the first band crossing have not been experimentally observed.

MeV appear to be sharper in the $\alpha = -\frac{1}{2}$ band. The same trends appear in the neighboring isotopes ^{77}Kr [19] and ^{81}Kr [4], although the $\alpha = -\frac{1}{2}$ bands are not known in the second crossing region.

The experimental Routhian curves in Fig. 6 show that the pattern of signature splittings is qualitatively similar in the yrast positive-parity bands of ^{79}Kr and neighboring nuclei. The signature splitting is larger at low frequencies, decreases to zero in the 1qp-3qp band crossing region, and increases again at higher frequencies. This behavior is understood in the Woods-Saxon cranking calculations [2,3] for the $N = 43$ isotones as a progression from a near-oblate shape for the $\nu g_{9/2}$ configuration through a near-prolate shape for the $\nu g_{9/2} \pi g_{9/2}^2$ configuration back to a near-oblate shape for the $\nu g_{9/2}^3 \pi g_{9/2}^2$ configuration. The present results on ^{79}Kr and the recent data on $^{81,83}\text{Sr}$ [5,11] provide some confirmation of the predicted second shape transformation.

Signature splitting in the level energies is often correlated with signature splitting in the $B(M1)$ transition strengths [20]. A strong alternation was seen [2] in the $B(M1)$ values for the yrast positive-parity band in ^{79}Kr for the low-spin states whose energies exhibit large signature splitting. However, above the 1qp-3qp band crossing in the region of vanishing signature splitting, the $B(M1)$ values become large and almost constant. Since the $B(E2)$ values generally vary smoothly,

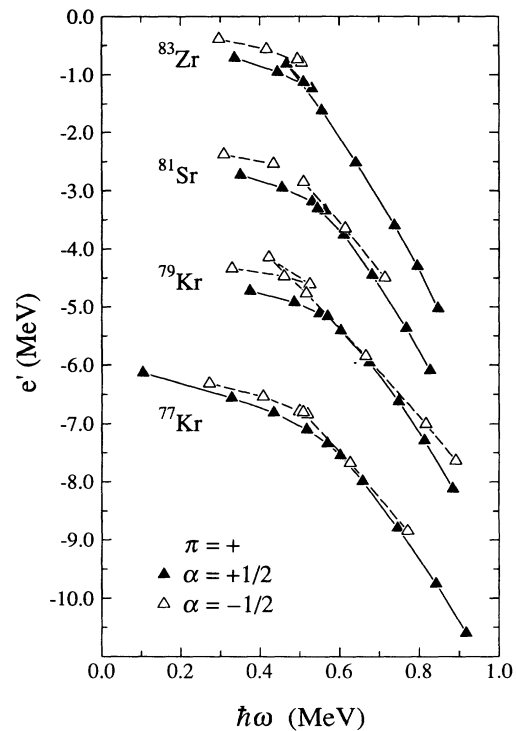


FIG. 6. Routhians e' versus rotational frequency $\hbar\omega$ for positive-parity states in ^{83}Zr [14-17], ^{81}Sr [3,11], ^{79}Kr , and ^{77}Kr [19,21,22]. Harris parameters $J_0 = 11 \hbar^2/\text{MeV}$ and $J_1 = 0 \hbar^3/\text{MeV}^4$ were used for the reference rotor. For the sake of clarity the data points for ^{81}Sr , ^{79}Kr , and ^{77}Kr have been artificially shifted by -2.0 , -4.0 , and -6.0 MeV, respectively.

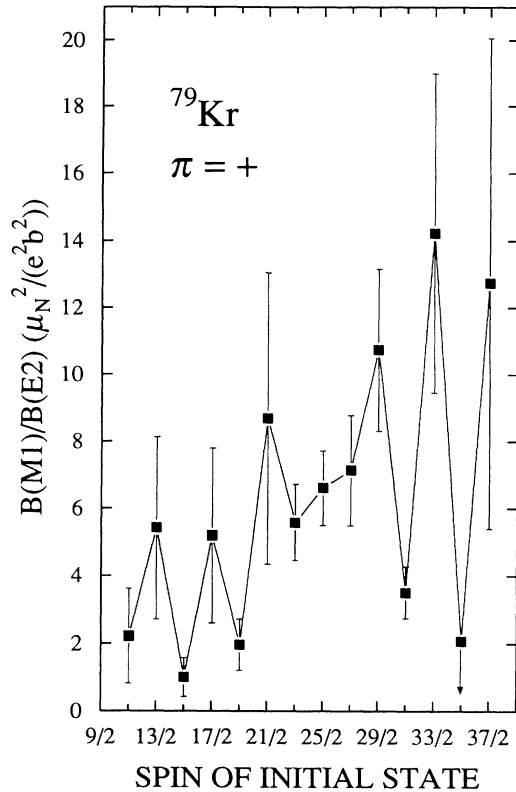


FIG. 7. Graph of $B(M1)/B(E2)$ ratio as a function of the spin of the initial state for the yrast positive-parity band in ^{79}Kr . A mixing ratio of $\delta = 0$ was used for the $\Delta I = 1$ transitions, although the results are not sensitive to δ as long as it is small.

the $B(M1)/B(E2)$ ratios also provide information on alternations in the $B(M1)$ strengths even when the lifetimes are not known. Such a graph is shown in Fig. 7 for the yrast positive-parity band in ^{79}Kr . This curve reproduces rather well the features previously reported for the absolute $B(M1)$ strengths. In addition, it shows a return to large $B(M1)$ alternations above the $27/2^+$ state in the region where the signature splitting increases again.

The kinematic moments of inertia in the yrast negative-parity band of ^{79}Kr (Fig. 8, top) increase rapidly with spin, but the three new points suggest a saturation at the rigid-body value. The dynamic moments of inertia (Fig. 8, bottom) show more clearly how the new points trace the completion of the band crossing at $\hbar\omega \approx 0.5$ MeV. Because this crossing occurs at the same frequency as in the positive-parity band, it was also interpreted [2] as a $\pi g_{9/2}$ alignment.

V. SUMMARY

High-spin states in ^{79}Kr were populated using the $^{65}\text{Cu}(^{18}\text{O}, p3n)$ reaction and their γ decays were observed with the Pitt-FSU detector array. The yrast positive-

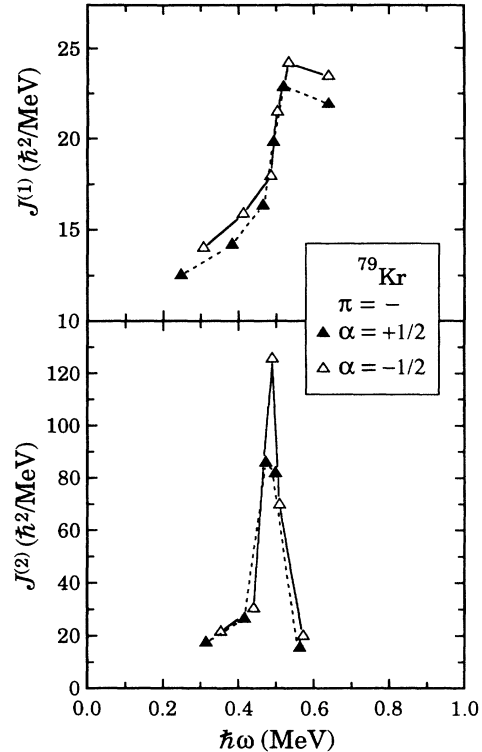


FIG. 8. Kinematic $J^{(1)}$ and dynamic $J^{(2)}$ moments of inertia as a function of rotational frequency $\hbar\omega$ for the yrast negative-parity band in ^{79}Kr .

parity band was extended up to the $(45/2^+)$ state, and the lowest negative-parity band up to the $(31/2^-)$ level. Spin assignments were made using the measured DCO ratios.

Some indications were seen for a second band crossing in the yrast band at $\hbar\omega \approx 0.75$ MeV, where similar evidence has also been seen in the adjacent nuclei $^{81,83}\text{Sr}$ and ^{83}Zr . The second alignment, probably due to $g_{9/2}$ neutrons, appears with a much larger band interaction than the first $g_{9/2}$ proton alignment. The increasing signature splitting above a frequency of 0.75 MeV/ \hbar is consistent with the theoretically predicted return to a near-oblate shape. Large alternations in the $B(M1)/B(E2)$ ratio also return with the signature splittings in the level energies.

The new states in the $K^\pi = \frac{5}{2}^-$ band confirm a band crossing at $\hbar\omega \approx 0.5$ MeV, which is expected to result from a $g_{9/2}$ proton alignment as in the positive-parity band.

ACKNOWLEDGMENTS

We are grateful to J.X. Saladin whose loan of the University of Pittsburgh detectors and electronics made the combined Pitt-FSU detector array possible. This work was supported in part by the National Science Foundation.

- [1] G. Winter, J. Döring, L. Funke, H. Prade, H. Rotter, R. Schwengner, A. Johnson, and A. Nilsson, *J. Phys. G* **14**, L13 (1988).
- [2] R. Schwengner, J. Döring, L. Funke, G. Winter, A. Johnson, and W. Nazarewicz, *Nucl. Phys.* **A509**, 550 (1990).
- [3] E.F. Moore, P.D. Cottle, C.J. Gross, D.M. Headly, U.J. Hüttmeier, S.L. Tabor, and W. Nazarewicz, *Phys. Rev. C* **38**, 696 (1988); *Phys. Lett. B* **211**, 14 (1988).
- [4] L. Funke, J. Döring, P. Kemnitz, E. Will, G. Winter, A. Johnson, L. Hildingsson, and Th. Lindblad, *Nucl. Phys.* **A455**, 206 (1986); *Phys. Lett.* **120B**, 301 (1983).
- [5] J. Döring, L. Funke, G. Winter, F. Lidén, B. Cedervall, A. Johnson, R. Wyss, J. Nyberg, and G. Sletten, in *Nuclear Structure in the Nineties*, edited by N. Johnson (Oak Ridge, Tennessee, 1990), p. 82.
- [6] J.S. Clements, L.R. Medsker, L.H. Fry, Jr., and L.V. Theisen, *Phys. Rev. C* **21**, 1285 (1980).
- [7] J. Lipták and J. Křištiak, *Nucl. Phys.* **A311**, 421 (1978).
- [8] M. Behar, A. Filevich, A.O. Macchiavelli, L. Szybisz, and P. Thieberger, *Phys. Rev. C* **26**, 1417 (1982).
- [9] G. Kajrys, S. Landsberger, R. Lecomte, and S. Monaro, *Phys. Rev. C* **27**, 983 (1983).
- [10] J. Panqueva, H.P. Hellmeister, L. Lühmann, F.J. Bergmeister, K.P. Lieb, and T. Otsuka, *Nucl. Phys.* **A389**, 424 (1982).
- [11] F. Lidén, J. Billowes, C. Mort, B.J. Varley, W. Gelletly, C.J. Gross, and D.D. Warner, *Daresbury Annual Report*, 1993, p. 7.
- [12] S.L. Tabor, M.A. Riley, J. Döring, P.D. Cottle, R. Books, T. Glasmacher, J.W. Holcomb, J. Hutchins, G.D. Johns, T.D. Johnson, T. Petters, O. Tekyi-Mensah, P.C. Womble, L. Wright, and J.X. Saladin, *Nucl. Instrum. Methods Phys. Res. Sect. B* **79**, 821 (1993).
- [13] S.L. Tabor, *Nucl. Instrum. Methods Phys. Res. Sect. A* **265**, 495 (1988).
- [14] U.J. Hüttmeier, C.J. Gross, D.M. Headly, E.F. Moore, S.L. Tabor, T.M. Cormier, P.M. Stwertka, and W. Nazarewicz, *Phys. Rev. C* **37**, 118 (1988).
- [15] S. Suematsu, Y. Haruta, B.J. Min, K. Heiguchi, Y. Ishikawa, S. Mitarai, T. Kuroyanagi, and Y. Onizuka, *Nucl. Phys.* **A485**, 304 (1988).
- [16] W. Fieber, K. Bharuth-Ram, J. Heese, F. Cristancho, C.J. Gross, K.P. Lieb, S. Skoda, and J. Eberth, *Z. Phys. A* **332**, 363 (1989).
- [17] D. Rudolph, C.J. Gross, K.P. Lieb, W. Gelletly, M.A. Bentley, H.G. Price, J. Simpson, B.J. Varley, J.L. Durell, Ö. Skeppstedt, and S. Rastikerdar, *Z. Phys. A* **338**, 139 (1991).
- [18] S.L. Tabor, *Phys. Rev. C* **45**, 242 (1992).
- [19] T.D. Johnson, J.W. Holcomb, P.C. Womble, P.D. Cottle, S.L. Tabor, F.E. Durham, S.G. Buccino, and M. Matsuzaki, *Phys. Rev. C* **42**, 2418 (1990).
- [20] G.B. Hagemann and I. Hamamoto, *Phys. Rev. C* **40**, 2862 (1989).
- [21] C.J. Gross, P.D. Cottle, D.M. Headly, U.J. Hüttmeier, E.F. Moore, S.L. Tabor, and W. Nazarewicz, *Phys. Rev. C* **36**, 2601 (1987).
- [22] B. Wörmann, K.P. Lieb, R. Diller, L. Lühmann, J. Keinonen, L. Cleemann, and J. Eberth, *Nucl. Phys.* **A431**, 170 (1984).